Neuron, Vol. 16, 1169–1177, June, 1996, Copyright ©1996 by Cell Press

Contribution of the S4 Segment to Gating Charge in the *Shaker* K^+ Channel

Sanjay Kumar Aggarwal and Roderick MacKinnon*
Department of Neurobiology
Harvard Medical School
Boston, Massachusetts 02115

Summary

Voltage-activated ion channels respond to changes in membrane voltage by coupling the movement of charges to channel opening. A K^+ channel-specific radioligand was designed and used to determine the origin of these gating charges in the *Shaker* K^+ channel. Opening of a *Shaker* K^+ channel is associated with a displacement of 13.6 electron charge units. Gating charge contributions were determined for six of the seven positive charges in the S4 segment, an unusual amino acid sequence in voltage-activated cation channels consisting of repeating basic residues at every third position. Charge-neutralizing mutations of the first four positive charges led to large decreases ($\sim$4 electron charge units each) in the gating charge; however, the gating charge of *Shaker* Δ10, a *Shaker* K^+ channel with 10 altered nonbasic residues in its S4 segment, was found to be identical to the wild-type channel. These findings show that movement of the NH_2-terminal half but not the CO_2H-terminal end of the S4 segment underlies gating charge, and that this portion of the S4 segment appears to move across the entire transmembrane voltage difference in association with channel activation.

Introduction

The voltage sensitivity of voltage-activated channels requires that charges in the membrane must move in response to membrane potential changes before the channels can open (Hodgkin and Huxley, 1952). These charges, known as gating charges, can be detected using electrophysiological methods (Armstrong and Bezanilla, 1973; Schneider and Chandler, 1973; Armstrong and Bezanilla, 1974; Keynes and Rojas, 1974), and their origin has been the subject of intense study. Voltage-activated cation channels contain an unusual amino acid sequence, the S4 segment, consisting of repeating basic residues (Arg or Lys) at every third position. The S4 segment has been proposed to function as a voltage sensor based on the uniqueness of this highly conserved region (Noda et al., 1984; Greenblatt et al., 1985; Kosower, 1985; Catterall, 1986; Guy and Seetharamulu, 1986; Noda et al., 1986). To test this hypothesis, researchers have neutralized positive charges in the S4 segment and attempted to measure a reduction in gating charge (Sthhmer et al., 1989; Liman et al., 1991; Lopez et al., 1991; Papazian et al., 1991; Logothetis et al., 1992; Tytgat and Hess, 1992; Logothetis et al., 1993). This reduction would represent the contribution of the positively charged residue to the gating charge of the channel.

The most obvious way to measure the gating charge of a single channel would be to record the gating current of a single channel using a patch clamp amplifier and integrate this current over time. Gating currents have an amplitude of about 1 fA per elementary charge when recorded through a system with an 8 kHz bandwidth (Sigg et al., 1994), about 1000-fold smaller than ionic currents. However, typical patch clamp systems have noise levels of around 100 to 200 fA RMS (Mika and Palti, 1994). Gating currents generated by a single channel are therefore lost in the noise generated from these patch clamp systems.

Gating charge in S4 mutant channels has been estimated as the product of a constant and the logarithmic change in the probability of channel opening at hyperpolarized potentials (Almers, 1978). Unfortunately, this measured slope of steady-state activation has been shown to determine inaccurately the gating charge of a channel (Schoppa et al., 1992; Sigworth, 1994; Zagotta et al., 1994). To test whether the S4 segment is a source of gating charge, we designed a K^+ channel-specific radioligand to count the number of channels expressed in a Xenopus oocyte. This allowed a measurement of total gating charge in an oocyte membrane to be converted into a determination of charge per channel.

Results

Synthesis of a K^+ Channel-Specific Radioligand

Agitoxin$_1$ ($AgTX_1$) is a high affinity inhibitor of the *Shaker* K^+ channel that blocks the channel with a stoichiometry of one to one (Garcia et al., 1994). A cassette containing a mutation of aspartate to cysteine at position 20 (D20C) was made by PCR mutagenesis and inserted into a T7 gene9 fusion expression vector (Park et al., 1991). Recombinant toxin was prepared as previously described (Garcia et al., 1994) and purified as disulfide-linked dimers, using reverse-phase high performance liquid chromatography (HPLC) (Figures 1A and 1B). Dimers were reduced with 10 mM dithiothreitol (DTT) and purified (Figure 1C). Reduced monomers were then alkylated using 45 μM tritiated *N*-ethylmaleimide ([^{3}H]NEM) (Shimony et al., 1994) and repurified as a single peak using HPLC (Figure 1D). Based on the extinction coefficient of nontritiated NEM-labeled $AgTX_1$D20C (ϵ_{235} = 8.88 $mM^{-1}cm^{-1}$), the specific activity of radiolabeled toxin was determined by measuring disintegrations per min (dpm) as a function of toxin concentration.

Characterization of Radioligand

Shaker K^+ channels were expressed in Xenopus oocytes and studied using a two-electrode voltage clamp. Figure 2A plots the fractional block of *Shaker* K^+ channels measured at different concentrations of unlabeled $AgTX_1$ (closed inverted triangles). Fraction of blocked current

*Present address: The Rockefeller University, 1230 York Avenue, New York, New York 10021.

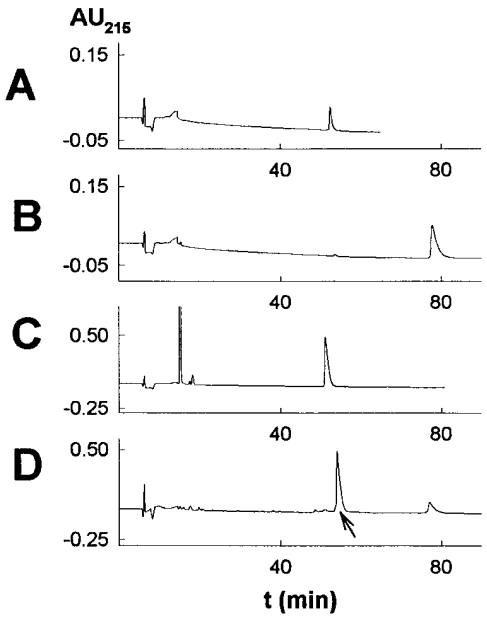

Figure 1. Synthesis and Purification of [^{3}H]NEM-Conjugated $AgTX_1D20C$

Reverse-phase HPLC chromatograms measured at a wavelength of 215 nM. Steps employed linear gradients from 0 to 35% mobile phase B over 2 min, 35% to 90% mobile phase B over 40 min, and 90% to 100% mobile phase B over 20 min. Mobile phase A was 0.1% trifluoroacetic acid (TFA) in water. Mobile phase B was 5% acetonitrile, 10% isopropanol, and 0.085% TFA in water.

(A) 200 pmoles of $AgTX_2$. The retention time of toxin was about 52.5 min.

(B) 500 pmoles of $AgTX_1D20C$ dimer. Toxin eluted at about 78 min.

(C) 5 nmoles of $AgTX_1D20C$ monomer following reduction of dimer by 10 mM DTT. Monomer eluted at about 51.7 min, about 25 min prior to the elution of dimer.

(D) 10 nmoles of $AgTX_1D20C$ monomer were reacted with 45 mM [^{3}H]NEM. Tritiated toxin eluted as a single peak from the column at about 54.3 min (arrow), 4 min later than unreacted monomer. Most of the $AgTX_1$ monomer reacted with either [^{3}H]NEM or redimerized.

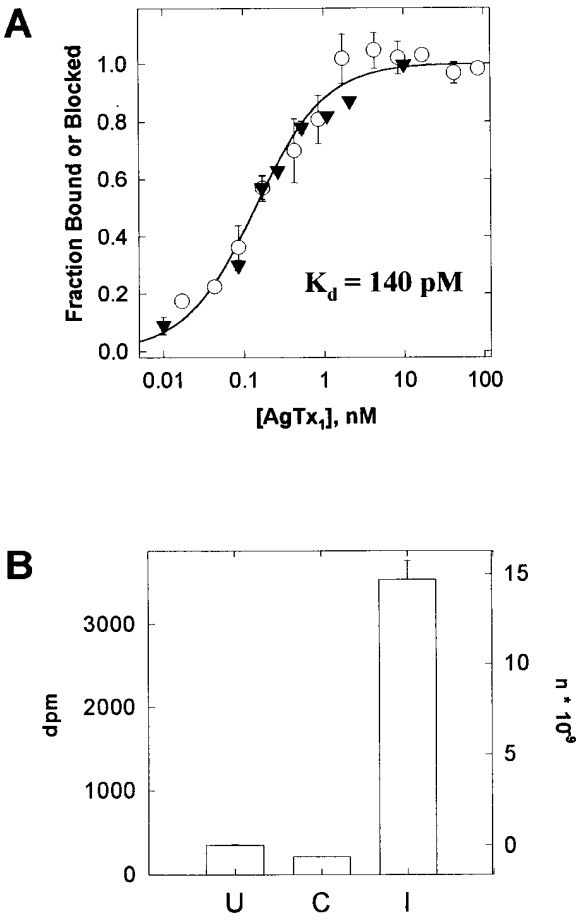

Figure 2. Characterization of [^{3}H]NEM-Conjugated $AgTX_1D20C$

(A) Fraction of channels bound by inhibitor (open circles) and fraction blocked (closed inverted triangles) at different concentrations of radiolabeled $AgTX_1D20C$ and unlabeled $AgTX_1$, respectively. Each binding point represents the mean ± SEM of 4 to 8 experiments, each experiment using 3–5 pooled oocytes. For the electrophysiological measurements, each point represents the mean ± SEM of 3 independent measurements. The curve corresponds to the fraction bound or blocked = $[T]/(K_d + [T])$, where K_d is the equilibrium dissociation constant and [T] is the toxin concentration.

(B) Tritiated $AgTX_1D20C$ binding data for oocytes expressing *Shaker* K^+ channels. The "U" bar represents uninjected oocytes (n = 3), "I" bar represents oocytes expressing channels (n = 5), and the "C" bar represents injected oocytes cotreated with a 40-fold greater concentration of unlabeled $AgTX_1$(n = 1). Histogram bars represent the mean dpm and mean number of channels (n). Error bars, shown for the "U" and "I" bars, represent the SEM. Bars "U" and "C" represent nonspecific binding. Dpm (left axis) was converted to channel number (right axis) by dividing specific binding (total binding minus nonspecific binding) by the specific activity of the radiolabeled toxin.

was the ratio of that measured in the presence to that in the absence of $AgTX_1$. The binding of radiolabeled $AgTX_1D20C$ was also studied at different toxin concentrations using a scintillation counter (open circles), and found to correlate well with the electrophysiological data. By fitting the data with a Langmuir adsorption isotherm, the equilibrium dissociation constant (K_d) of radiolabeled $AgTX_1D20C$ was determined to be about 140 pM. Also, the dissociation time constant of NEM-conjugated $AgTX_1D20C$ (as measured by two-electrode voltage clamp and binding studies) was nearly identical to that of native $AgTX_1$ (approximately 12 min, data not shown). These data indicate that the characteristics of radiolabeled $AgTX_1D20C$-binding are indistinguishable from those of unlabeled $AgTX_1$ conductance inhibition. Therefore, the D20C mutation and NEM-conjugation do not interfere with the interaction of the toxin and the channel.

Figure 2B shows binding data obtained for a typical batch of oocytes. Uninjected oocytes (bar "U") and injected oocytes cotreated with a 40-fold greater concentration of unlabeled $AgTX_1$ (bar "C") were used to determine nonspecific binding. The total number of *Shaker* K^+ channels expressed for an oocyte was then calculated by dividing the specific binding by the specific activity of the radiolabeled toxin. For this batch, an average of 14.7 billion *Shaker* K^+ channels were expressed per oocyte (bar "I"). Dividing mean total binding (bar "I") by the mean nonspecific binding, a signal-to-noise ratio of about 13 was calculated for this measurement.

Determination of the Gating Charge of the *Shaker* K^+ Channel

Using recombinant agitoxin$_2$ ($AgTX_2$, an isoform of $AgTX_1$) (Garcia et al., 1994) to block ionic current, capacitive currents were measured in Xenopus oocytes expressing *Shaker* K^+ channels (Figure 3A). $AgTX_2$ was used instead of $AgTX_1$, because $AgTX_2$ dissociates 12 times faster than $AgTX_1$ and could therefore be removed more quickly from the channels after electrophysiological measurements.

The repolarization-induced (or "off") capacitive currents were integrated over time to yield a charge versus voltage (Q-V) plot (Figure 3B). The linear components of this plot (dashed lines) represent the linear capacitance of the cell and voltage clamp system, while the nonlinear component reflects gating charge movement of *Shaker* K^+ channels. The same total gating charge was obtained when integrating either the repolarization-induced or the depolarization-induced (or "on") capacitive currents. Therefore, gating charge was never found to be immobilized by the pulse potentials (Bezanilla et al., 1991). Capacitive currents were also measured for uninjected oocytes (Figure 3C). The Q-V plot (Figure 3D) derived from uninjected oocytes was linear, indicating that oocytes do not possess significant native sources of nonlinear charge displacement.

After measuring capacitive currents in an oocyte expressing *Shaker* K^+ channels, the oocyte was rinsed several times and then perfused for 20 min to remove bound $AgTX_2$ (dissociation time constant of about 1 min). Oocytes were then treated with 85 nM [^{3}H]NEM-$AgTX_1$D20C to determine total channel number. Plotting the gating charge as a function of channel number for many oocytes yielded a correlation plot (Figure 3E). Each point in this plot represents a different oocyte, and each set of symbols (circles, squares, triangles, and inverted triangles) represent measurements made with independent radiolabeled toxin preparations. Deviations of measured charge per channel among these different radiolabeled toxin preparations are representative of the error in the measurement of their specific activities. As can be seen, these deviations were relatively small. Fitting the data with a linear regression, the slope, or charge per channel, was determined to be about 13.6 electron charge units for the *Shaker* K^+ channel. This number is similar to the charge per channel of 12.4, measured using nonstationary fluctuation analysis (Schoppa et al., 1992). The fact that these two independent methods are in agreement implies that the binding of $AgTX_2$ to the channel does not alter its gating charge, and that there is a one-to-one correspondence between the ability to bind toxin and move gating charge.

Contribution of Basic Residues in the S4 Segment to Gating Charge

The amino acid sequence of the *Shaker* K^+ channel S4 segment is shown with the seven positively charged residues bold-faced and numbered (Figure 4A). Mutations were made at each of these seven positively charged residues, and were assayed for functional expression in Xenopus oocytes (Table 1). No charge-altering mutations at position 6 produced functional channels. Mutations in the S4 segment were not found to

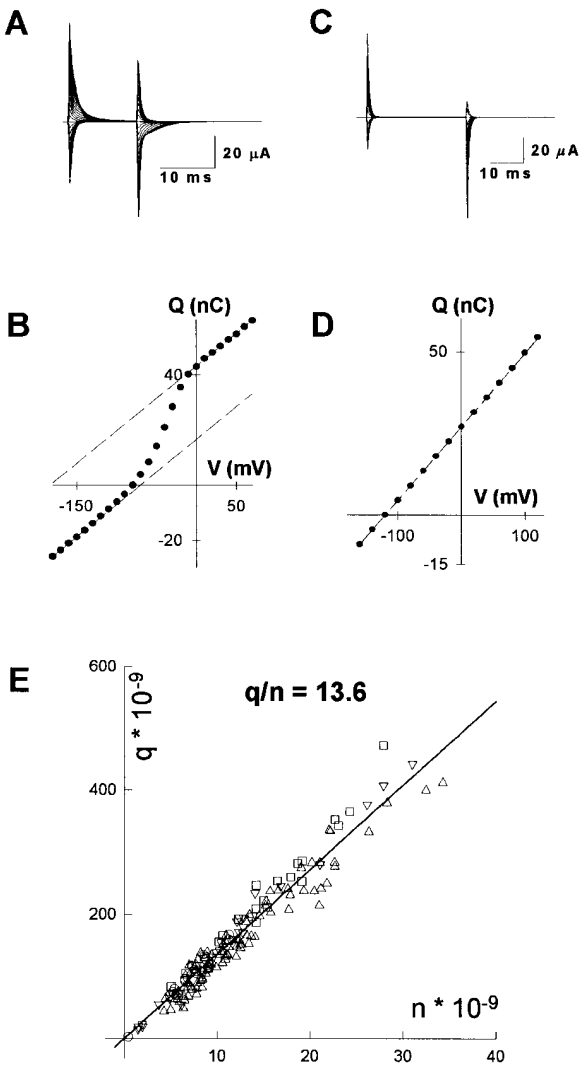

Figure 3. Determination of the Gating Charge of the *Shaker* K^+ Channel

(A) Using at least 50 μM of $AgTX_2$ to block ionic current (at least 105-fold higher than its K_d for the *Shaker* K^+ channel), capacitive currents were measured for an oocyte expressing *Shaker* K^+ channels.

(B) Repolarization-induced currents were integrated over time to give total charge, and plotted as a function of pulse potential (Q-V plot). The linear components of this plot (dashed lines) represent the linear capacitance of the cell and voltage clamp system, while the nonlinear component reflects gating charge movement.

(C) Capacitive currents measured for an uninjected oocyte.

(D) Q-V plot of repolarization-induced currents is linear. Xenopus oocytes do not possess significant endogenous sources of nonlinear charge displacement.

(E) Correlation plot mapping total gating charge (q) in electron charge units as a function of total channel number (n) for several oocytes expressing *Shaker* K^+ channels. Total channel number was determined by binding oocytes with 85 nM tritiated $AgTX_1$D20C. Each point represents a different oocyte ($n = 162$), and each set of symbols (circles, squares, triangles, and inverted triangles) represent measurements made with independent radiolabeled toxin preparations. The line corresponds to a linear regression fit using the methods of least squares with a slope, or charge per channel (q/n), of 13.6 electron charge units. The 95% confidence interval for this measurement is ± 0.2 electron charge units.

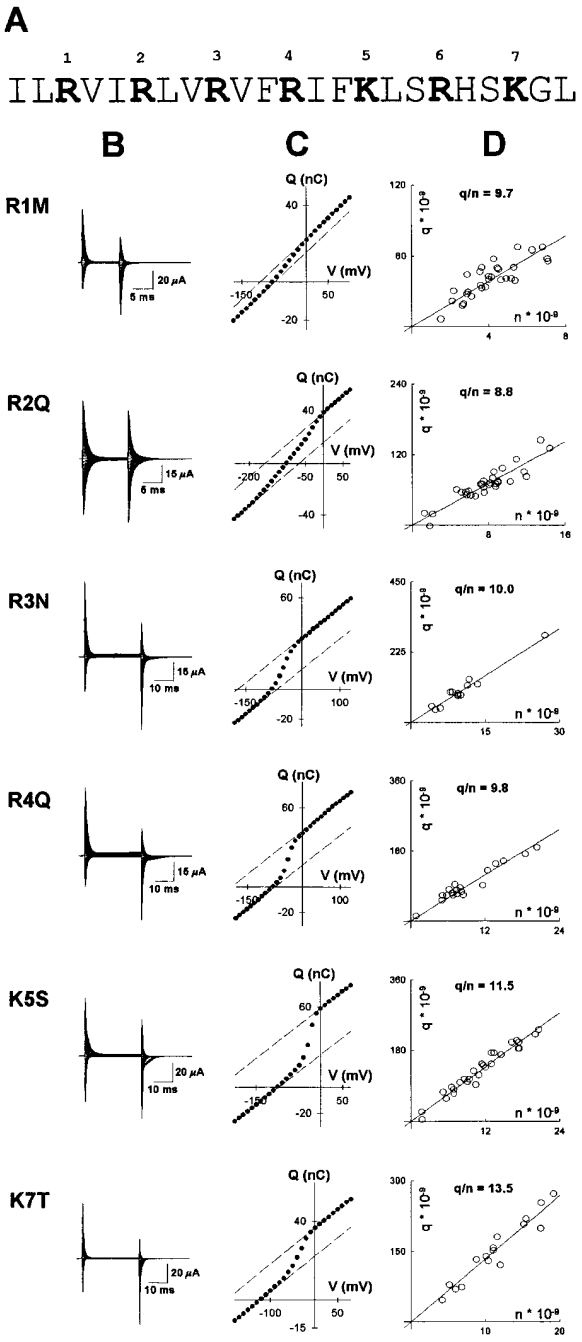

Figure 4. Determination of Gating Charge for Charge-Neutralizing Mutations in the S4 Segment

(A) The amino acid sequence of the *Shaker* K^+ channel's S4 segment, with basic residues bold-faced and numbered. Mutagenesis was performed at each of these seven positive charges. For the unmodified *Shaker* K^+ channel, R1 corresponds to amino acid position 362.

(B–D) Capacitive currents (B), Q-V plots (C), and correlation plots (D) mapping total gating charge (q) in electron charge units as a function of total channel number (n) for the following S4 mutations: R1M (n = 30), R2Q (n = 30), R3N (n = 15), R4Q (n = 20), K5S (n = 28), and K7T (n = 16). Channel number was normalized (see text). The lines in the correlation plots correspond to linear regression fits of the data.

alter significantly $AgTX_1$ and $AgTX_2$-binding. Therefore, we were able to use the assay to determine the gating charge of several of these mutant channels. Capacitive currents (Figure 4B), Q-V plots (Figure 4C), and charge per channel correlation plots (Figure 4D) are shown for the charge-neutralizing mutations R1M, R2Q, R3N, R4Q, K5S, and K7T. Charge-neutralizing mutations at positions 1, 2, 3, and 4 decreased gating charge by about 4 electron charge units. K5S decreased it by 2 electron charge units, and K7T had no effect.

Capacitive currents (Figure 5A), Q-V plots (Figure 5B), and charge per channel correlation plots (Figure 5C) are shown for the charge-conserving mutations R1K, R2K, R3K, and K5R. These mutations either did not significantly change the measured charge per channel (positions 2 and 3) or increased it by about 2 electron charge units (positions 1 and 5).

For these S4 mutant channels, the same total gating charge was obtained when integrating either the repolarization-induced or the depolarization-induced capacitive currents. Therefore, gating charge was never found to be immobilized by the pulse potentials (Bezanilla et al., 1991). As discussed above, a systematic error was introduced into these charge per channel measurements by the accuracy at which the specific activity of a given radiolabeled toxin preparation could be measured. This error was relatively small (Figure 3E), and was corrected by calculating a normalized channel number $N' = N \times (G_{WT}/G'_{WT})$ for each oocyte, where N was the uncorrected channel number; G_{WT} was gating charge of the wild-type *Shaker* K^+ channel, as measured in parallel that same day using identical radiolabeled toxin preparations and identical recording solutions; and G'_{WT} was the gating charge of the *Shaker* K^+ channel, as measured over all days (13.6, Figure 3E).

Contribution of Nonbasic Residues in the S4 Segment to Gating Charge

To test whether gating charge perturbation is specific to the mutation of charged residues in the S4 segment, noncharged residues were also mutated. *Shaker* Δ10 (Figure 6A) is a *Shaker* K^+ channel, with 10 nonbasic residues changed to those found in the S4 segment of a related K^+ channel, drk1 (Frech et al., 1989). While the Q-V relationship of *Shaker* Δ10 (Figure 6B) was very different from that of the wild-type *Shaker* K^+ channel, the charge per channel was unaltered (Figure 6C). This implies that the magnitude of gating charge is dependent on charged and not uncharged residues in the S4 segment.

Discussion

Alterations in charge per channel are summarized for all S4 charge mutations (Figures 7A–7C). One property of these data is that individual charge perturbations do not add up exactly. For example, the total sum of effects resulting from the six neutralizing mutations equals 18.3, not 13.6. If a charge-neutralizing mutation affected only the electric charge at that site and no other properties of the protein, then the sum should be less than or equal

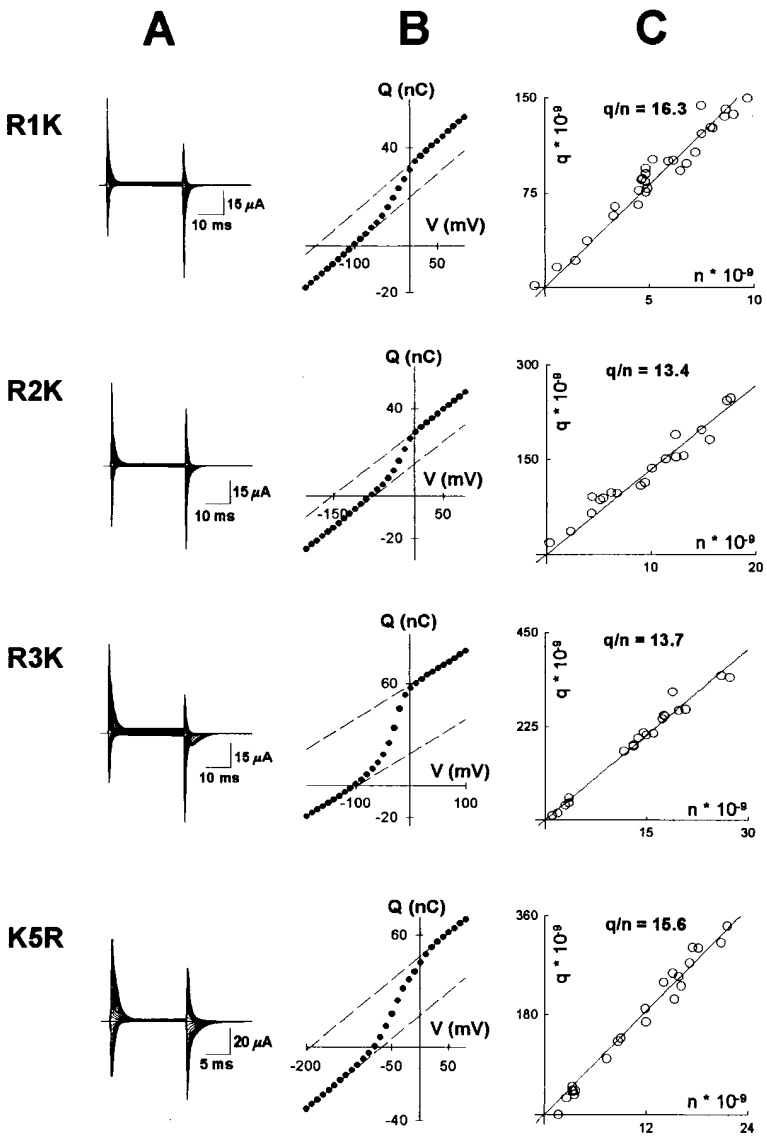

Figure 5. Determination of Gating Charge for Charge-Conserving Mutations in the S4 Segment

Capacitive currents (A), Q-V plots (B), and correlation plots (C) mapping total gating charge (q) in electron charge units, as a function of total channel number (n) for the following S4 mutations: R1K (n = 29), R2K (n = 19), R3K (n = 20), and K5R (n = 22). Channel number was normalized (see text). The lines in the correlation plots correspond to linear regression fits of the data.

to 13.6. As this is not the case, other properties, such as the positions of neighboring charged residues, must be affected by at least some of these mutations. Another example of nonadditivity is given by the two mutations at position 1: the difference in gating charge between R1K and R1M is 7, rather than 4 (that would be expected if this residue contributes one charge per subunit) (MacKinnon, 1991; Hurst et al., 1992; Liman et al., 1992; Li et al., 1994). The lack of additivity observed here is not surprising, because an electric charge is expected to affect the distribution of neighboring charges if they are mobile. Amino acid side chains are not as mobile as free molecules in solution, but they are not fixed rigidly in space, either. Therefore, a charge-neutralizing mutation removes a charge (a primary effect) and, to some unknown extent, redistributes neighboring charges (a secondary effect). Both effects may contribute to the measured difference in total gating charge brought about by a mutation.

From the above discussion, it follows that a change in gating charge can not be interpreted simply as a function of distance that the mutated residue moves through the membrane voltage difference. Nevertheless, the data argue that the effects of the mutations are intimately connected to this region's role as a voltage sensor. Specifically, only charge-neutralizing mutations reduce the gating charge significantly. This conclusion is most impressively shown by the *Shaker* Δ10 mutation (10 altered hydrophobic residues; Figures 6 and 7C), where the voltage dependence of charge movement is extremely abnormal but the total quantity of gating charge is the same as for the wild-type channel.

Even though we are unable to break down the effect of a mutation into its primary (loss of the charge itself) versus secondary (redistribution of neighboring charges) components, the quantity of gating charge-change associated with mutation of R1 through R4 implies that the primary component dominates. For each of these sites, the charge change is not far from four. This number may be a coincidence, but we think it more likely reflects

Table 1.

Amino Acid	R1*	R2*	R3*	R4*	K5*	R6*	K7*
A	+	+			+	−	
C	+				−	−	
D							
E							
F					−	−	
G	+				+	−	
H							
I					−	−	
K	+	+	+	+	(wt)	+	(wt)
L					−	−	
M	+	+			+	−	
N			+		−	−	
P							
Q	+	+		+	−	−	
R	(wt)	(wt)	(wt)	(wt)	+	(wt)	
S		+			+	−	
T	+	+			+	−	+
V	+				−	−	
W	+				−	−	
Y					−	−	

the fact that each charge from R1 to R4 moves all the way across the transmembrane voltage difference in all four subunits when the channel gates. Therefore, the conformational change associated with channel opening would involve the transfer of at least a 10 amino acid segment across the voltage difference for each subunit. This would require an even larger conformational change than has been implicated by cysteine-labeling studies (Larsson et al., 1996; Mannuzzu et al., 1996).

Movement of the S4 segment may be similar to that demonstrated in the bacteriocidal protein colicin, in which a large segment of peptide is transferred across the entire membrane upon channel activation (Slatin et al., 1994). Most likely, such a transition would involve a change in secondary structure (Sigworth, 1994). For example, the S4 segment might form a helix in one state of the channel and a loop in another state (Figure 7D). Helix-to-loop transitions have been described to occur in other proteins upon activation (e.g., in the BamHI endonuclease when binding to DNA; Newman et al., 1995). Such a model seems more likely than one in which the S4 segment moves across the membrane as a sliding helix, with no break in secondary structure (Durell and Guy, 1992).

Experimental Procedures

Shaker K+ Channel Expression

The *Shaker* K^+ channel clone used in this study was the *Shaker* H4 construct (Kamb et al., 1988) in a BlueScript vector. Amino acids 6–46 were deleted to remove fast (N-type) inactivation (Hoshi et al., 1990). Amino acid numbering refers to the unmodified channel. Xenopus oocytes were harvested from mature female Xenopus laevis (Xenopus One, Ann Arbor, MI; Nasco, Fort Atkinson, WI). Oocytes were placed in a saline solution (82.5 mM NaCl, 2.5 mM KCl, 1.0 mM $MgCl_2$, 5 mM HEPES, [pH 7.6]) with 2–3 mg/ml of Type II collagenase (Worthington) and dissociated at 120 rpm for about 2 hr, rinsed thoroughly, and stored in ND96 solution (96 mM NaCl, 2 mM KCl, 1.8 mM $CaCl_2$, 1.0 mM $MgCl_2$, 5 mM HEPES, 50 μg/ml gentamicin [pH 7.6]). Defolliculated oocytes were selected at least 2 hr after collagenase treatment, and were injected with RNA. RNA was prepared by linearizing the *Shaker* H4 K^+ channel plasmid with

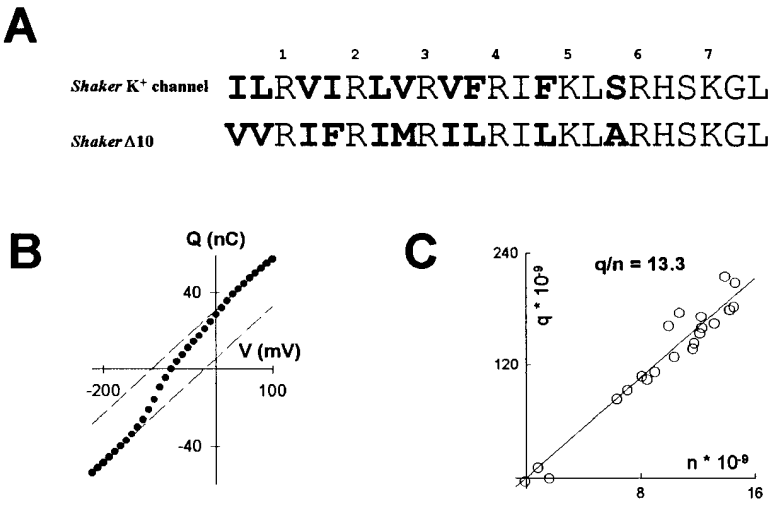

Figure 6. Contribution of Nonbasic Residues in the S4 Segment to Gating Charge

(A) The amino acid sequence of the S4 segment in the *Shaker* K^+ channel and the *Shaker* Δ10 mutant channel. All basic amino acid residues are numbered. Mutated nonbasic residues are bold-faced.

(B) Q-V plots of repolarization-induced currents for an oocyte.

(C) Correlation plots mapping total gating charge (q) in electron charge units as a function of total channel number (n) (n = 21). Channel number was normalized (see text). The line corresponds to a linear regression fit of the data. The gating charge of *Shaker* Δ10 is not significantly different from that of the wild-type channel.

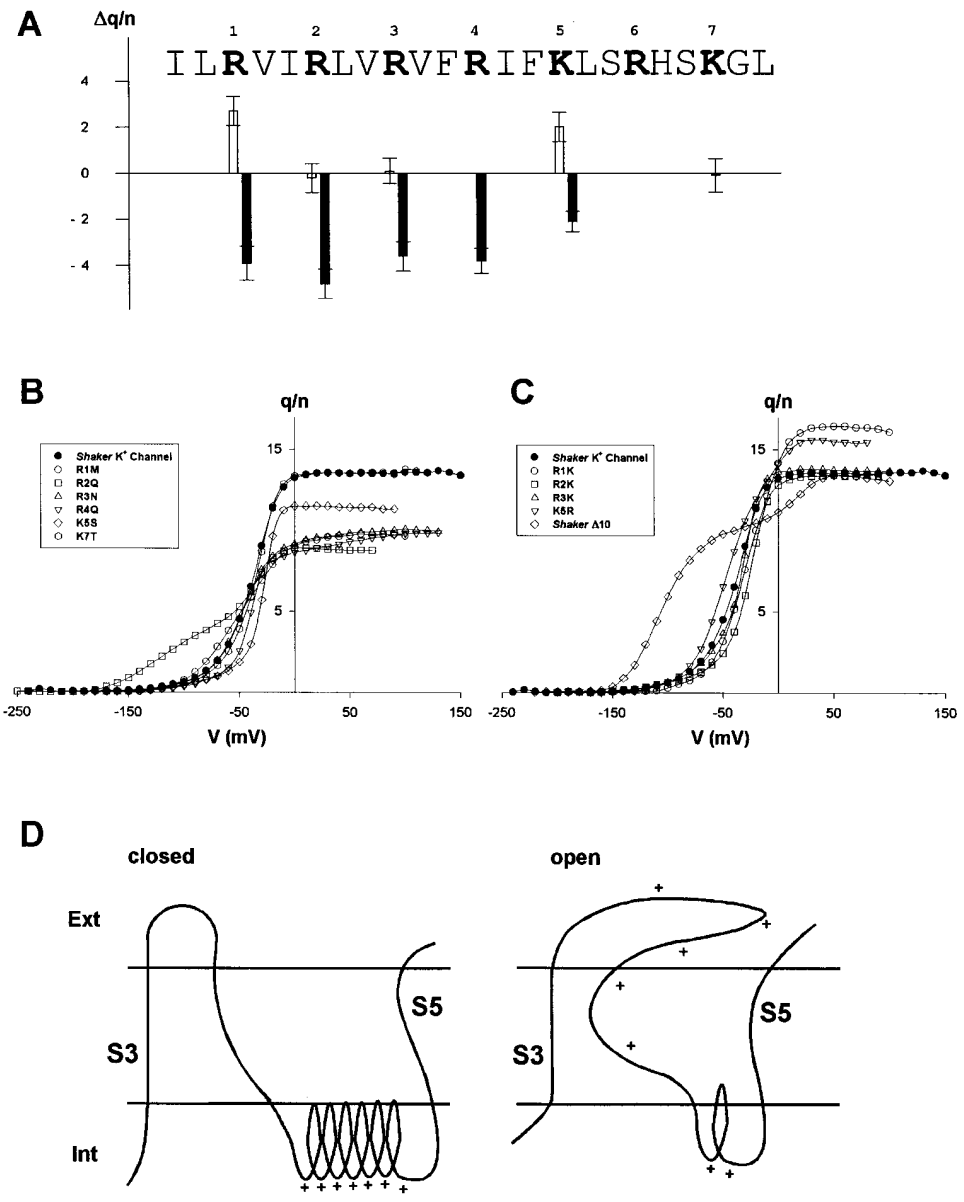

Figure 7. Summary

(A) Change in the gating charge (Δ q/n) of charge-conserving (open bars) and -neutralizing (closed bars) S4 mutations relative to that of the wild-type *Shaker* K^+ channel. Bars are aligned with the basic residues mutated in the S4 segment of the *Shaker* K^+ channel. A positive Δ q/n indicates that the mutant has more gating charge than the wild-type *Shaker* K^+ channel, while a negative Δ q/n indicates less gating charge. Error bars represent the 95% confidence intervals for these measurements.

(B and C) Gating charge movement (q/n) for the wild-type *Shaker* K^+ channel and charge-neutralizing (B) and charge-conserving (C) S4 mutations as a function of pulse potential (V). For an S4 mutant channel, data points represent the mean gating charge movement measured in all oocytes used to determine its charge per channel (Figures 4, 5, or 6). For the wild-type *Shaker* K^+ channel, a representative selection of oocytes were used ($n = 22$). Only oocytes expressing at least 2×10^9 channels were included.

(D) A model of *Shaker* K^+ channel gating, in which the S4 segment undergoes a change in secondary structure. The S4 segment is shown for both the closed and the open states of the channel. "Ext" and "Int" denote the extracellular and intracellular sides of the membrane, respectively.

HindIII and transcribing in vitro using T7 RNA polymerase. Injection of oocytes 36–48 hr postharvest was found to yield an optimal level of K^+ channel expression. Also, $AgTX_2$ at a concentration of about 500 nM (1000-fold greater than its K_d for the *Shaker* K^+ channel) was often added to the incubation media following RNA injection. This treatment allowed injected oocytes to survive about twice as long and express at least twice as many channels as oocytes not treated with $AgTX_2$, and reduced leak current by several fold when studied under two-electrode voltage clamp.

Electrophysiological Recording

Currents were recorded using a two-electrode voltage clamp amplifier under computer control at room temperature, and filtered at 1–5 kHz with an 8 pole Bessel filter. To measure ionic currents, oocytes were held at −80 mV and pulsed to 0 mV for 50 ms as described (Garcia et al., 1994). Recording solution contained 96 mM NaCl, 2 mM KCl, 0.3 mM $CaCl_2$, 1.0 mM $MgCl_2$, and 5 mM HEPES (pH 7.6). We added 50 μg/ml bovine serum albumin (BSA) to minimize nonspecific binding of the toxin. When measuring capacitive currents,

holding and repolarization potentials were between −80 and −120 mV, with pulse potentials starting between -160 and −250 mV and ending between +70 and +150 mV in 10 to 20 mV increments. Either solution A or solution B was used for a given oocyte. Solution A was identical to recording solution, except that it contained no BSA. Solution B contained 100 mM *N*-methyl-D-glucamine (NMDG), 0.3 mM $CaCl_2$, 1.0 mM $MgCl_2$, and 5 mM HEPES (pH 7.6). The substitution of NMDG, a relatively impermeable cation, for Na^+ and K^+ dramatically reduced the amplitude of both leak and inward and outward rectifying currents. Charge per channel measurements made in solution A and solution B were not significantly different and were combined. Typically, 2–5 hr elapsed between the measurement of capacitive currents and labeling with tritiated $AgTX_1D20C$.

Binding Assay

Binding studies were performed with at least a 20-fold excess of radiolabeled-toxin compared to the total number of *Shaker* K^+ channels present on a given oocyte. When oocytes were treated with low concentrations of tritiated $AgTX_1D20C$, the volume of binding solution was expanded to meet this requirement. The binding solution was identical to recording solution, except it contained 1 mg/ml BSA. Oocytes were treated with radiolabeled $AgTX_1D20C$ for at least 60 min (for the *Shaker* K^+ channel, this is equivalent to about 5 dissociation time constants) at room temperature. Unbound radiolabeled toxin was washed off the oocyte in 20 s or less (less than 3% of the dissociation time constant), using two to four rinses of quench buffer, each rinse equivalent to about a 1:1000 dilution. The quench buffer contained 200 mM NaCl and 20 mM HEPES (pH 7.4). Each oocyte was then placed in a scintillation vial containing 500 μl of 1% SDS and vortexed. We added 5 ml of scintillation fluid to each vial, and radioactivity was assayed using a scintillation counter.

Only oocytes that prevented radiolabeled toxin from passing across their membranes were used. To select for these oocytes, several injected oocytes from each Xenopus laevis frog were incubated in 85 nM tritiated $AgTX_1D20C$ for 1 hr (the typical period of a binding assay in a charge per channel measurement). Labeled toxin was then displaced from the K^+ channels by incubating the oocytes for over 3 hr in 1 μM unlabeled $AgTX_1$. Using this protocol, radiolabeled toxin was completely displaced from oocytes in approximately 90% of all batches. The 10% of batches that allowed toxin entry were not used. This protocol was carried out every time a binding assay was done, and therefore excluded the possibility of occult toxin internalization.

Mutagenesis

Mutations in the S4 segment were generated by second strand synthesis on a single-strand version of the plasmid or by PCR mutagenesis. In both cases, a region of DNA containing the mutant was subcloned into *Shaker* K^+ channel DNA and sequenced.

Acknowledgments

We would like to thank M. L. Garcia for measuring the extinction coefficient of nontritiated NEM-labeled $AgTX_1D20C$; F. J. Sigworth, Z. Lu, and K. J. Swartz for helpful discussions; and A. Lee and V. R. Aggarwal for their continued support throughout the course of this work. S. K. Aggarwal was supported by NRSA fellowship (MH10989) awarded by the National Institute of Mental Health. This research was supported by awards from the PEW Charitable Trust and McKnight Foundation in Neuroscience.

The costs of publication of this article were defrayed in part by the payment of page charges. This article must therefore be hereby marked *"advertisement"* in accordance with 18 USC Section 1734 solely to indicate this fact.

Received March 15, 1996; revised April 12, 1996.

References

Almers, W. (1978). Gating currents and charge movements in excitable membranes. Rev. Physiol. Biochem. Pharmacol. *82*, 96–190.

Armstrong, C.M., and Bezanilla, F. (1973). Currents related to movement of the gating particles of the sodium channels. Nature *242*, 459–461.

Armstrong, C.M., and Bezanilla, F. (1974). Charge movement associated with the opening and closing of the activation gates of the Na channels. J. Gen. Physiol. *63*, 533–552.

Bezanilla, F., Perozo, E., Papazian, D.M., and Stefani, E. (1991). Molecular basis of gating charge immobilization in *Shaker* potassium channels. Science *254*, 679–683.

Catterall, W.A. (1986). Molecular properties of voltage-sensitive sodium channels. Annu. Rev. Biochem. *55*, 953–985.

Durell, S.R., and Guy, H.R. (1992). Atomic scale structure and functional models of voltage-gated potassium channels. Biophys. J. *62*, 238–250.

Frech, G.C., VanDongen, A.M.J., Schuster, G., Brown, A.M., and Joho, R.H. (1989). A novel potassium channel with delayed rectifier properties isolated from rat brain by expression cloning. Nature *340*, 642–645.

Garcia, M.L., Garcia-Calvo, M., Hidalgo, P., Lee, A., and MacKinnon R. (1994). Purification and characterization of three inhibitors of voltage-dependent K^+ channels from *Leiurus quinquestriatus* var. *hebraeus* venom. Biochemistry *33*, 6834–6839.

Greenblatt, R.E., Blatt, Y., and Montal, M. (1985). The structure of the voltage-sensitive sodium channel. Inferences derived from computer-aided analysis of the *Electrophorus electricus* channel primary structure. FEBS Lett. *193*, 125–134.

Guy, H.R., and Seetharamulu, P. (1986). Molecular model of the action potential sodium channel. Proc. Natl. Acad. Sci. USA *83*, 508–512.

Hodgkin, A.L., and Huxley, A.F. (1952). A quantitative description of membrane current and its application to conduction and excitation in nerve. J. Physiol. *117*, 500–544.

Hoshi, T., Zagotta, W.N., and Aldrich, R.W. (1990). Biophysical and molecular mechanisms of *Shaker* potassium channel inactivation. Science *250*, 533–538.

Hurst, R.S., Kavanaugh, M.P., Yakel, J., Adelman, J.P., and North, R.A. (1992). Cooperative interactions among subunits of a voltage-dependent potassium channel. J. Biol. Chem. *267*, 23742–23745.

Kamb, A., Tseng-Crank, J., and Tanouye, M.A. (1988). Multiple products at the *Drosophila shaker* gene may contribute to potassium channel diversity. Neuron *1*, 421–430.

Keynes, R.D., and Rojas, E. (1974). Kinetics and steady-state properties of the charged system controlling sodium conductance in the squid giant axon. J. Physiol. *239*, 393–434.

Kosower, E.M. (1985). A structural and dynamic molecular model for the sodium channel of *Electrophorus electricus*. FEBS Lett. *182*, 234–242.

Larsson, H.P., Baker, O.S., Dhillon, D.S., and Isacoff, E.Y. (1996). Transmembrane movement of the *Shaker* K^+ channel S4. Neuron *16*, 387–397.

Li, M., Unwin, N., Stauffer, K.A., Jan, Y.-N., and Jan, L.Y. (1994). Images of purified *Shaker* potassium channels. Curr. Biol. *4*, 110–115.

Liman, E.R., Hess, P., Weaver, F., and Koren, G. (1991). Voltage-sensing residues in the S4 region of a mammalian K^+ channel. Nature *353*, 752–756.

Liman, E.R., Tytgat, J., and Hess, P. (1992). Subunit stoichiometry of a mammalian K^+ channel determined by construction of multimeric cDNAs. Neuron *9*, 861–871.

Logothetis, D.E., Movahedi, S., Satler, C., Lindpaintner, K., and Nadal-Ginard, B. (1992). Incremental reductions of positive charge within the S4 region of a voltage-gated K^+ channel result in corresponding decreases in gating charge. Neuron *8*, 531–540.

Logothetis, D.E., Kammen, B.F., Lindpaintner, K., Bisbas, D., and Nadal-Ginard, B. (1993). Gating charge differences between two voltage-gated K^+ channels are due to the specific charge content of their respective S4 regions. Neuron *10*, 1121–1129.

Lopez, G.A., Jan, Y.-N., and Jan, L.Y. (1991). Hydrophobic substitution mutations in the S4 sequence alter voltage-dependent gating in *Shaker* K^+ channels. Neuron *7*, 327–336.

MacKinnon, R. (1991). Determination of the subunit stoichiometry of a voltage-activated potassium channel. Nature *350*, 232–235.

Mannuzzu, L.M., Moronne, M.M., and Isacoff, E.Y. (1996). Direct physical measure of conformation rearrangement underlying potassium channel gating. Science *271*, 213–216.

Mika, Y.H., and Palti, Y. (1994). Charge displacements in a single potassium ion channel macromolecule during gating. Biophys. J. *67*, 1455–1463.

Newman, M., Strzelecka, T., Dorner, L.F., Schildkraut, I., and Aggarwal, A.K. (1995). Structure of Bam HI endonuclease bound to DNA: partial folding and unfolding on DNA binding. Science *269*, 656–663.

Noda, M., Shimizu, S., Tanabe, T., Takai, T., Kayano, T., Ikeda, T., Takahashi, T, Nakayama, H., Kanaoka, Y., Minamino, N., Kangawa, K., Matsuo, H., Raftery, M.A., Hirose, T., Inayama, S., Hayashida, H., Miyata, T., and Numa, S. (1984). Primary structure of *Electrophorus electricus* sodium channel deduced from cDNA sequence. Nature *312*, 121–127.

Noda, M., Ikeda, T., Kayano, T., Suzuki, H., Takeshima, H., Kurasaki, M., Takahashi, H., and Numa, S. (1986). Existence of distinct sodium channel messenger RNAs in rat brain. Nature *320*, 188–192.

Papazian, D.M., Timpe, L.C., Jan, Y.N., and Jan, L.Y. (1991). Alteration of voltage-dependence of *Shaker* potassium channel by mutations in the S4 sequence. Nature *349*, 305–310.

Park, C.-S., Hausdorff, S.F., and Miller, C. (1991). Design, synthesis, and functional expression of a gene for charybdotoxin, a peptide blocker of K^+ channels. Proc. Natl. Acad. Sci. USA *88*, 2046–2050.

Schneider, M.F., and Chandler, W.K. (1973). Voltage-dependent charge movement in skeletal muscle: a possible step in excitation-contraction coupling. Nature *242*, 244–246.

Schoppa, N.E., McCormack, K., Tanouye, M.A., and Sigworth, F.J. (1992). The size of gating charge in wild-type and mutant *Shaker* potassium channels. Science *255*, 1712–1715.

Shimony, E., Sun, T., Kolmakova-Partensky, L., and Miller, C. (1994). Engineering a uniquely reactive thiol into a cysteine-rich peptide. Protein Eng. *7*, 503–507.

Sigg, D., Stefani, E., and Bezanilla, F. (1994). Gating current noise produced by elementary transitions in *Shaker* potassium channels. Science *264*, 578–582.

Sigworth, F.J. (1994). Voltage gating of ion channels. Q. Rev. Biophys. *27*, 1–40.

Slatin, S.L., Qiu, X.-Q., Jakes, K.S., and Finkelstein, A. (1994). Identification of a translocated protein segment in a voltage-dependent channel. Nature *371*, 158–161.

Stühmer, W., Conti, F., Suzuki, H., Wang, X.D., Noda, M., Yahagi, N., Kubo, H., and Numa, S. (1989). Structural parts involved in activation and inactivation of the sodium channel. Nature *339*, 597–603.

Tytgat, J., and Hess, P. (1992). Evidence for cooperative interactions in potassium channel gating. Nature *359*, 420–423.

Zagotta, W.N., Hoshi, T., Dittman, J., and Aldrich, R.W. (1994). *Shaker* potassium channel gating II: transitions in the activation pathway. J. Gen. Physiol. *103*, 279–319.